Search for large-scale anisotropy of ultra-high energy cosmic rays with the Telescope Array first year data

P. Tinyakov[*†], H. Koers[*], O. Kalashev[†], H. Kang[‡], S. Ogio[§], and G. Thomson[¶] for the Telescope Array Collaboration

[*]*Service de Physique Théorique, Université Libre de Bruxelles (U.L.B.), Belgium*
[†]*Institute for Nuclear Research of the Russian Academy of Sciences, Russia*
[‡]*Department of Earth Sciences, Pusan National University, Korea*
[§]*Graduate School of Science, Osaka City University, Japan*
[¶]*Department of Physics and Astronomy, Rutgers - The State University of New Jersey, USA*

***Abstract*. We report on a study of large-scale anisotropy of arrival directions of ultra-high energy cosmic ray events collected by the surface detector of the Telescope Array in the first year of operation. In particular, we investigate correlations of cosmic ray events with the matter distribution in the nearby Universe.**

***Keywords*: Telecope Array, UHECR anisotropies, large-scale structure.**

I. Introduction

The observed cutoff in the spectrum of ultra-high energy cosmic rays (UHECR) at an energy of order 5×10^{19} eV [1], [2] suggests that cosmic rays of the highest energies come from the nearby Universe, i.e. from distances within 100–200 Mpc. Because the matter distribution is inhomogeneous on these scales, the flux of the highest energy cosmic rays observed on Earth is expected to be anisotropic. The distribution of flux over the sky can be calculated in different models of UHECR production and propagation. Comparing this to observations then allows us to discriminate between models and to determine their key astrophysical parameters.

The Telescope Array (TA) detector [3], being the largest cosmic-ray experiment in the Northern hemisphere, will offer a unique insight into the distribution of cosmic-ray sources. It consists of 507 ground-array detectors and three fluorescent telescopes overlooking the ground array. TA has started full operation in spring 2008. In this work we present an anisotropy analysis of data collected by the TA surface detectors during the period from April to November 2008.

The strength and character of the anisotropy in the UHECR flux depends crucially on two parameters: the source density and the amplitude of deflections in Galactic and extragalactic magnetic fields. The deflections in turn depend on the strength and correlation length of the magnetic fields, and on charges and energies of the primary particles. The deflections may vary from a few degrees for protons to many tens of degrees for heavy nuclei. In a large class of realistic models the number of sources is large, while the deflections of UHECR are relatively small. This situation is envisaged in the "matter tracer" model, a benchmark model that is (apart from details on the injection spectrum to which the pattern of arrival directions is not very sensitive) characterized by a single parameter, the typical deflection angle $\theta_{\rm s}$. In this study we consider two models: the matter tracer model and an isotropic source distribution (hereafter the "isotropy" model). Note that, as $\theta_{\rm s}$ becomes very large, the model predictions of the matter tracer model will become close to those of an isotropic source distribution. Consequently it will be increasingly difficult to discriminate between the two models. Consistent with the assumption of relatively small deflections in the matter tracer model, we assume a proton composition of UHECR in this study.

The comparison between the first year TA data and model predictions is done by the "flux sampling" method that was introduced in Ref. [4]. This method has several advantages. It does not require binning, which makes it statistically unambiguous. Moreover it has stronger discriminative power than traditional methods based on a two-dimensional Kolmogorov-Smirnov (KS) test or a χ^2-test.

In the following we describe our model and the flux sampling method in detail; results and conclusions will be presented at the ICRC.

II. Method

A. Modeling of flux and exposure

The flux sampling method requires as input the sky map of predicted flux modulated with experimental exposure. We express the exposure-modulated flux from galactic longitude l and latitude b with energy above E as $\tilde{\Phi}(l,b,E) \equiv \Phi(l,b,E)\,\Xi(l,b,E)$, where Φ denotes the integral cosmic-ray flux and Ξ the experimental exposure. At energies larger than 10 EeV the TA efficiency is close to unity, so that the exposure may be approximated as geometrical:

$$\Xi(\delta) \propto \sin\eta(\xi)\cos\delta\cos\delta_{\rm TA} + \eta(\xi)\sin\delta\sin\delta_{\rm TA}\,, \quad (1)$$

where δ denotes the declination in J2000 equatorial coordinates; $\delta_{\rm TA} = 39.3^\circ$ is the TA declination; $\xi \equiv (\cos\theta_{\rm m} - \sin\delta_{\rm TA}\sin\delta)/(\cos\delta_{\rm TA}\cos\delta)$; and the function $\eta(\xi) \equiv \arccos\xi$ for $|\xi| \le 1$, while $\eta(\xi) \equiv \pi$ for $\xi < -1$ and $\eta(\xi) \equiv 0$ for $\xi > 1$. In the above $\theta_{\rm m} = 45^\circ$ denotes the maximum zenith angle of the events.

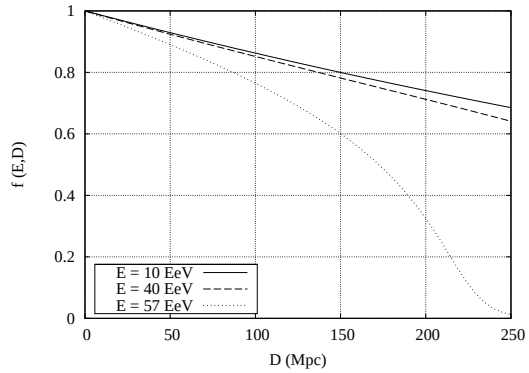

Fig. 1. The function $f(E, D)$, which parameterizes the effect of UHECR energy loss due to redshift and attenuation, as a function of source distance D for different values of threshold energy E.

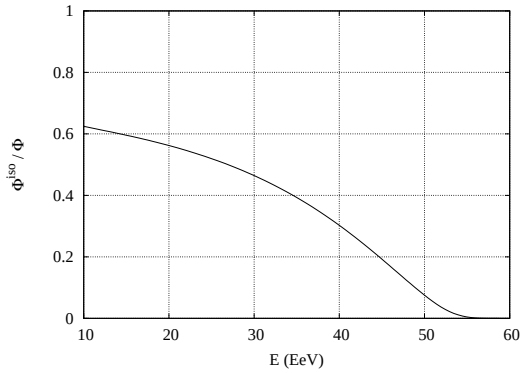

Fig. 2. The ratio $\Phi^{\rm iso}/\Phi$ (both integrated over the sky), indicating the relative strength of the flux $\Phi^{\rm iso}$ that is added to account for sources beyond 250 Mpc, where the galaxy catalog is cut.

The cosmic-ray flux is modeled from a galaxy catalog, essentially using galaxies as tracers of the large-scale distribution of matter. We express:

$$\Phi = \sum_i \Phi_i w_i^{\rm cat} w_i^{\rm s} + \Phi^{\rm iso}\,, \qquad (2)$$

where Φ_i denotes the integral flux from galaxy i, $w_i^{\rm cat}$ is the weight assigned to galaxy i in the catalog (see below), $w_i^{\rm s}$ is a weight that depends on the angle between galaxy i and the line of sight, and $\Phi^{\rm iso}$ is an isotropic flux that accounts for sources outside the galaxy catalog. In the following these terms are considered in more detail. The flux from an individual source is expressed as follows:

$$\Phi_i = \frac{f(E, D_i) J(E)}{4\pi D_i^2}\,, \qquad (3)$$

where J denotes the integral injection spectrum , which we take to be a universal power-law $J \propto E^{-1.2}$ extending to very high energies (we treat all sources as equal); D_i is the source distance; and f is a factor that accounts for energy loss due to redshift and particle interactions between the source and the Earth. This factor is determined numerically using the propagation code that is described in Ref. [4]. It is shown in figure 1 as a function of distance for three different threshold energies.

The angular weight $w_i^{\rm s}$ essentially replaces a point-source flux by a probability density distribution so as to account for UHECR deflections in Galactic and intergalactic magnetic fields. It also accounts for limited angular resolution of the experiment and prevents unphysical fluctuations due to the use of a catalog of point sources. We adopt a weight $w_i^{\rm s} \propto \exp(-\theta^2/\theta_{\rm s}^2)$, where θ denotes the angle between galaxy i and the line of sight and $\theta_{\rm s}$ is the smearing angle.

The galaxy catalog adopted in the present study is a tailored sample of the 2 Micron All-Sky Redshift Survey (2MRS) [5], a flux-limited sample of galaxies with observed K_s-magnitude $m \leq 11.25$ that contains spectroscopic redshifts for all but a few galaxies.[1] The galactic plane has been removed in the sample by cutting away all galaxies with $|b| < 10^\circ$. Since the 2MRS represents a flux-limited sample it contains preferentially nearby galaxies. To compensate for this selection effect, every galaxy is assigned a distance-dependent weight $w_i^{\rm cat}$. A detailed description of these weights, together with an algorithm to compute them from a given catalog with maximum accuracy, will be presented elsewhere.

The isotropic flux component $\Phi^{\rm iso}$ is added by hand to account for sources beyond the maximum distance in the catalog (where we assume a homogeneous source distribution). We have truncated the 2MRS sample at 250 Mpc, where the catalog becomes too sparse to provide an accurate statistical description. The strength of the UHECR flux from sources beyond this distance, which depends on energy, is calculated using the UHECR propagation routine described in Ref. [4]. The result is shown in figure 2.

The distribution of exposure-modulated flux over the sky is shown in figure 3 for different energies. The flux maps exhibit a stronger contrast (and hence a stronger deviation from isotropy) with increasing energy, reflecting the increasing importance of nearby structures due to the decreasing UHECR horizon. Some prominent structures may be recognized in the maps, notably the center of the Virgo cluster at $\sim$20 Mpc and the Perseus-Pisces supercluster at $\sim$70 Mpc.

B. Statistical test

The compatibility of a model source distribution with a set of UHECR arrival directions is quantified by the method introduced in Ref. [4], to which we will refer as the flux sampling method. In summary, the method is based on correlating a set of model flux values from a "test" event set (either real data or mock events) with a "reference" set that is representative of the model to be tested. The flux values are obtained by sampling a model flux map (such as the map shown in fig. 3), i.e. by extracting flux values at specific points on the sphere. These points may represent the arrival directions of observed UHECR or may be generated according to the model to be tested. The "test" and "reference" sets of

[1] This sample was kindly provided to us by John Huchra.

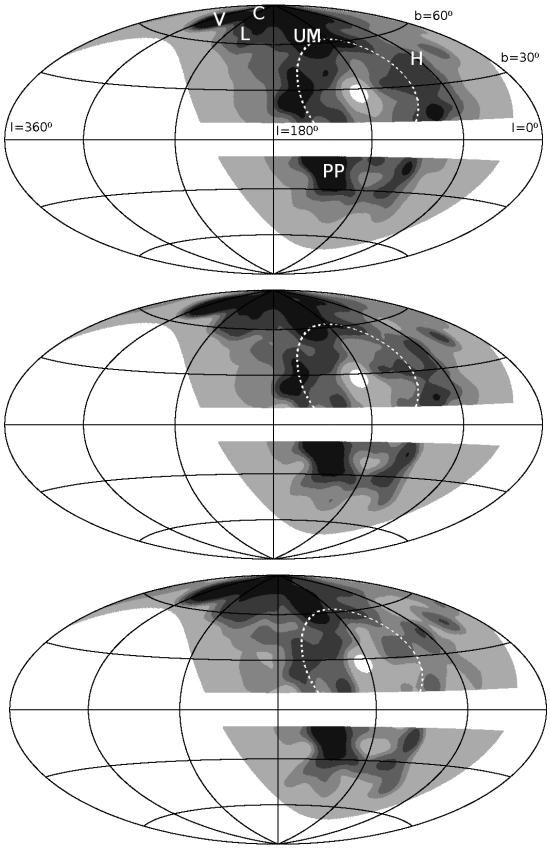

Fig. 3. Aitoff projection of the sky (galactic coordinates) showing the expected UHECR flux above 10 EeV (top panel), 40 EeV (middle), and 57 EeV (bottom), modulated with experimental exposure. Darker gray indicates a higher flux, with the division in bands such that every band integrates to 1/5 of the total exposure-modulated flux. The white area shows the region outside the TA field of view and the galactic plane, which has been removed from the 2MRS catalog. The dashed white curve indicates where the exposure is maximal. Some prominent structures (clusters and superclusters) are indicated: Coma (C), Hercules (H), Leo (L), Perseus-Pisces (PP), Ursa Major (UM), and Virgo (V). In producing these figures we have adopted a smearing angle $\theta_{\rm s} = 6^\circ$.

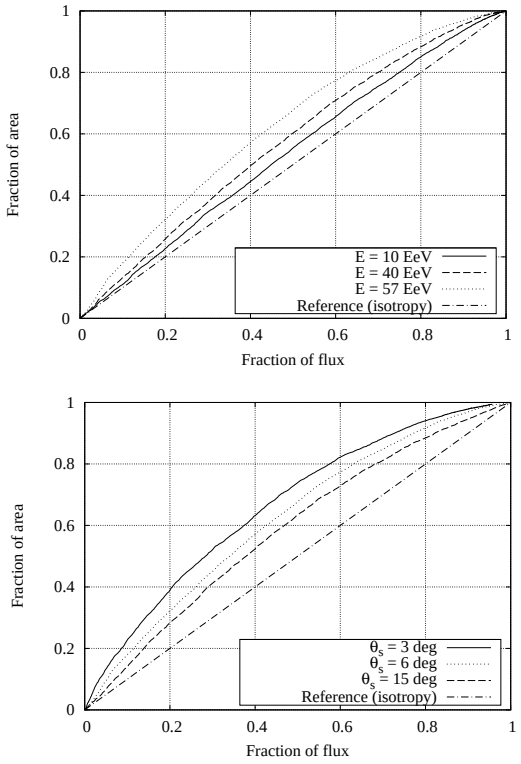

Fig. 4. Fraction of the area (corrected for exposure) on the sphere occupied by regions up to a limiting flux (relative to the maximum flux in the model). Top panel: varying threshold energy E with $\theta_{\rm s} = 6^\circ$; bottom panel: varying $\theta_{\rm s}$ with $E = 57$ EeV.

flux values are correlated by a standard KS test or by an asymmetric variation of this test introduced in Ref. [4]. In the former case this yields a test statistic D; in the latter case we denote the resulting test statistic as Y. The relevant statistical quantities, in particular powers and p-values, are computed from the distribution of the test statistics D and Y.

An intuitive way to think about flux distributions over the sky is in terms of the area that is occupied by a certain range of flux values. For the matter tracer model, regions of high flux will be relatively concentrated while regions of small flux will occupy a relatively large area on the sphere. For an isotropic source distribution, the distribution of flux over the sphere will be more uniform. This effect is shown in figure 4, where we plot the cumulative area distribution against the cumulative flux distribution (going from small to large values, and with all distributions normalized to unity). The difference between the model distributions underlies the flux sampling method (essentially, the test samples these distributions and compares them by a KS test). The figure clearly demonstrates how the contrasts, and hence the deviation from isotropy, increase with increasing threshold energy and decreasing smearing angle.

As a way of assessing the potential of the proposed test, we consider the number of events required for a power $P = 0.5$ (i.e., a 50% probability) to rule out (at 95% CL) a source distribution tracing the distribution of matter when the true distribution is isotropic. The resulting number of events is shown in figure 5 as a function of $\theta_{\rm s}$ for threshold energies 10 EeV, 40 EeV, and 57 EeV. The figure clearly demonstrates how the necessary number of events increases with increasing smearing angle and with decreasing energy, reflecting the increasing similarity between predictions of the matter tracer model and the isotropy model. (We stress that these results are theoretical forecasts which are independent of the actual data.) The typical number of events indicated in figure 5, namely a few hundred above 10 EeV and a few tens above 57 EeV, can be accumulated with TA within roughly a year.

III. Results and conclusions

Results will be presented at the ICRC, together with the conclusions drawn from them.

The central result will be an assessment of the (in)compatibility between TA data on the one hand and model predictions for an isotropic source distribution and for a source distribution tracing the distribution

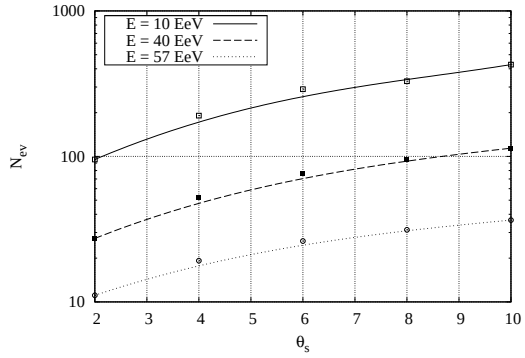

Fig. 5. Number of events $N_{\rm ev}$ required for a 50% probability to rule out, at 95% CL, a source distribution tracing the distribution of matter when the true distribution is isotropic, plotted as a function of smearing angle $\theta_{\rm s}$. The points are results from the flux sampling method; the curves are a smooth interpolation. The figure applies to the D-test (the corresponding figure for the Y-test is similar).

of matter in the Universe on the other hand. The (in)compatibility is quantified as a p-value, giving the probability that the model yields an outcome at least as extreme as what has been observed. For the case of a source distribution tracing the distribution of matter, we scan over $\theta_{\rm s}$ to establish which (if any) values are in contradiction with the data.

A possible improvement on this work is to model the source distribution and the angular deflection at the level of individual events (as opposed to using a model flux map and smearing angle at the threshold energy). This would capture correlations between the CR horizon and the smearing angle on one hand, and the energy (and, possibly, the direction) of individual CR events on the other. Because these correlations contain additional information on the source distribution, including them may improve the discriminatory power of the test.

ACKNOWLEDGEMENTS

The Telescope Array experiment is supported by the Ministry of Education, Culture, Sports, Science and Technology-Japan through Kakenhi grants on priority area (431) “Highest Energy Cosmic Rays”, basic research awards 18204020(A), 18403004(B) and 20340057(B); by the U.S. National Science Foundation awards PHY-0601915, PHY-0703893, PHY-0758342, and PHY-0848320 (Utah) and PHY-0649681 (Rutgers); by the Korean Science and Engineering Foundation (KOSEF, Grant No. R01-2007-000-21088-0); by the Russian Academy of Sciences, RFBR grants 07-02-00820a and 09-07-00388a (INR); by the FNRS under contract 1.5.335.08, IISN, and BSP under IUAP VI/11 (ULB). The foundations of Dr. Ezekiel R. and Edna Wattis Dumke, Willard L. Eccles and the George S. and Dolores Dore Eccles all helped with generous donations. The State of Utah supported the project through its Economic Development Board, and the University of Utah through the Office of the Vice President for Research. The experimental site became available through the cooperation of the Utah School and Institutional Trust Lands Administration (SITLA), U.S. Bureau of Land Management and the U.S. Air Force. We also wish to thank the people and the officials of Millard County, Utah, for their steadfast and warm support. We gratefully acknowledge the contributions from the technical staffs of our home institutions.

REFERENCES

[1] Abbasi, R. *et al.* [HiRes Collaboration], *Observation of the GZK cutoff by the HiRes experiment*, Phys. Rev. Lett. **100**, 101101 (2008)

[2] Abraham, J. *et al.* [Pierre Auger Collaboration], *Observation of the suppression of the flux of cosmic rays above* 4×10^{19} *eV*, Phys. Rev. Lett. **101**, 061101 (2008)

[3] Tokuno, H. *et al.* [Telescope Array Collaboration], *The Telescope Array experiment: Status and prospects*, J. Phys. Conf. Ser. **120**, 062027 (2008)

[4] Koers, H. B. J. and Tinyakov, P., *Testing large-scale (an)isotropy of ultra-high energy cosmic rays*, JCAP **0904**, 003 (2009)

[5] Huchra, J., Macri, L., Jarrett, T., Martimbeau, N., Masters, K., Crook, A., Cutri, R., Schneider, S. and Skutskie, M., in preparation (2009)